ELSEVIER

Journal of Alloys and Compounds 374 (2004) 84–88

Journal of ALLOYS AND COMPOUNDS

www.elsevier.com/locate/jallcom

Characterization and thermal behavior of amorphous rare earth phosphates

Hidekazu Hirai [a], Toshiyuki Masui [a], Nobuhito Imanaka [a,*], Gin-ya Adachi [b]

[a] *Department of Applied Chemistry, Faculty of Engineering and Handai Frontier Research Center, Osaka University, 2-1 Yamadaoka, Suita, Osaka 565-0871, Japan*

[b] *Juri Institute for Environmental Science and Chemistry, College of Analytical Chemistry, 2-1-8 Temma, Kita-ku, Osaka 530-0043, Japan*

Abstract

Amorphous cerium and terbium pyrophosphates were synthesized by precipitation method at 353 K. The characterization of these amorphous phosphates was carried out by using X-ray powder diffraction (XRD), thermal gravimetric and differential thermal analysis (TG–DTA), Fourier-transformed infrared spectroscopy (FT-IR), and Raman spectroscopy, especially focusing on the thermal behavior dependence on the calcination temperatures. The amorphous state of the as-prepared cerium phosphate was stable up to 723 K, and it crystallized at 773 K to form a mixture of cerium pyrophosphate (CeP_2O_7) and cerium orthophosphate ($CePO_4$). Heating at higher temperatures accelerates the phase change from pyrophosphate to orthophosphate accompanying the formation of metaphosphate (CeP_3O_9), and above 1173 K, only a single phase of $CePO_4$ was obtained. In the case of terbium phosphate, crystallization of amorphous phase occurred at 973 K to produce a mixture of $TbPO_4$ and $Tb_2P_4O_{13}$. The $Tb_2P_4O_{13}$ phase decomposed into TbP_3O_9 and $TbPO_4$ at 1673 K, and these compounds remained even after the calcination at 1873 K.

Keywords: Rare earth phosphates; Amorphous; X-ray diffraction; Thermal analysis; FT-IR; Raman

1. Introduction

In recent years, much attention has been paid to the rare earth phosphates because of their potential applications for optical materials, including laser [1], phosphors [2], and more recently, anti-UV materials [3]. Although the latter materials utilized their amorphous features for ultraviolet shielding, there were few basic and systematic studies on the thermal behavior of amorphous rare earth phosphates [4,5].

In the series of rare earth elements, cerium and terbium can form their tetravalent ions as well as trivalent ones, and it is very interesting to identify the most stable phases at the lowest temperature which causes crystallization in these phosphates. In addition, characterization of the thermal behavior of these amorphous phosphates, especially on the structural changes with heating, is very important for several applications.

In this study, amorphous cerium and terbium phosphates were prepared by precipitation method, respectively, to investigate their thermal behavior in details using X-ray powder diffraction (XRD), thermal gravimetric and differential thermal analysis (TG–DTA), Fourier-transformed infrared spectroscopy (FT-IR), and Raman spectroscopy.

2. Experimental procedure

2.1. Preparation of amorphous cerium phosphate

Cerium(IV) sulfate tetrahydrate was dissolved in deionized water and the concentration was adjusted to $1.0\,mol\,dm^{-3}$. A $0.1\,mol\,dm^{-3}$ of sodium pyrophosphate aqueous solution was used as a precipitant. These solutions were mixed and the precipitate was agitated with magnetic stirrer for 30 min at 353 K. The particles obtained were separated by centrifuging, washed with deionized water five times, and dried at 353 K for 24 h. Then the powders were calcined in air at 473, 723, 773, 823, 873, 923, 973, 1023, 1173, and 1373 K for 5 h at a heating rate of $100\,K\,h^{-1}$.

2.2. Preparation of amorphous terbium phosphate

Terbium(III) sulfate octahydrate was dissolved in $1.0\,mol\,dm^{-3}$ sulfuric acid and the concentration of Tb^{3+}

---

[*] Corresponding author.

E-mail address: imanaka@chem.eng.osaka-u.ac.jp (N. Imanaka).

0925-8388/$ – see front matter © 2003 Elsevier B.V. All rights reserved.
doi:10.1016/j.jallcom.2003.11.069

ion was adjusted to 1.0 mol dm^{-3}. The solution was dropped into a 0.1 mol dm^{-3} of sodium pyrophosphate aqueous solution, and then the final pH value was adjusted to 5 with a 3.0 mol dm^{-3} of ammonium hydroxide solution. After stirring for 30 min at 353 K, the particles were separated by centrifuging, washed with deionized water and acetone, and dried at room temperature for 24 h. The powders obtained were calcined in air at 873, 973, 1073, 1373, 1423, 1473, 1673, and 1873 K for 5 h at a heating rate of 100 K h^{-1}.

2.3. Characterization of the amorphous cerium and terbium phosphates

The compositions of the samples were determined by an X-ray fluorescent spectrometer (Rigaku ZEX-100e). The XRD data were obtained on an X-ray diffractmeter (Rigaku Multiflex) with Cu Kα radiation. FT-IR (JASCO FTIR-430) and Raman spectra (Kaiser Optical Systems, HoloProbe) were recorded for both samples. TG–DTA analysis was carried out at a heating rate of 10 K min^{-1} (Shimadzu DTG-60H).

3. Results and discussion

3.1. Thermal behavior of the amorphous cerium phosphate

The XRD patterns of the as-prepared and calcined cerium phosphate samples were summarized in Fig. 1. The samples heated at low temperatures below 723 K were amorphous. After the calcination at 753 K, the crystallization of the amorphous cerium phosphate occurred and a mixture of the crystalline cerium pyrophosphate (CeP_2O_7) and cerium orthophosphate ($CePO_4$) was formed. Structural change of the cerium pyrophosphate into cerium orthophosphate was promoted by heating at higher temperatures, accompanying with the formation of cerium metaphosphate (CeP_3O_9). Finally, a single phase of $CePO_4$ was obtained at 1373 K.

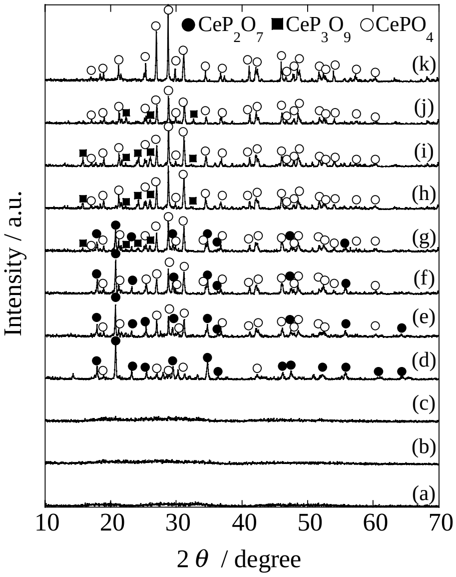

Fig. 1. XRD patterns of cerium phosphate calcined at various temperatures: as-prepared (a), calcined at 473 K (b), 723 K (c), 773 K (d), 823 K (e), 873 K (f), 923 K (g), 973 K (h), 1023 K (i), 1173 K (j), and 1373 K (k).

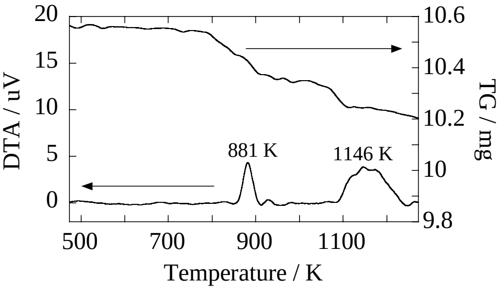

Fig. 2. TG–DTA spectra of cerium phosphate dried at 473 K.

TG–DTA spectra of the amorphous CeP_2O_7 dehydrated at 473 K are shown in Fig. 2. Both the weight loss and an exothermic peak were observed at 881 K. This exothermic weight loss corresponded to the change from CeP_2O_7 to both CeP_3O_9 and $CePO_4$ with the evolution of oxygen gas [4]. Another exothermic broad peak in the DTA curve and the corresponding weight loss were also observed at 1146 K, which were attributed to the change from CeP_3O_9 to $CePO_4$ [4].

The FT-IR spectra of the as-prepared and calcined cerium phosphate samples are illustrated in Fig. 3. In the FT-IR spectra of amorphous cerium phosphate [5], four distinct bands were observed at 1070, 925, 622, and 522 cm^{-1}. The main band at 1070 cm^{-1} was due to the asymmetric

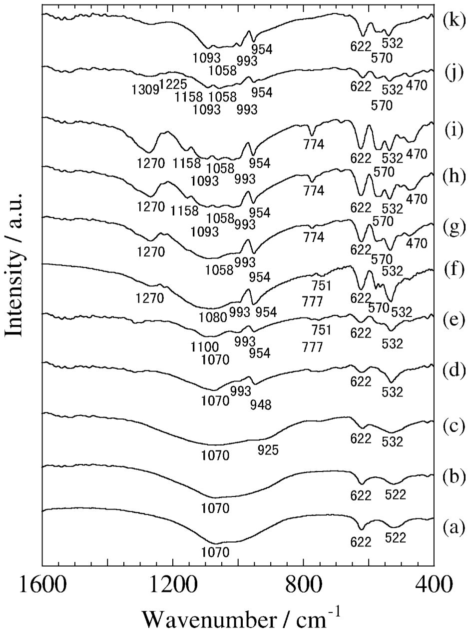

Fig. 3. FT-IR spectra of cerium phosphate calcined at various temperatures: as-prepared (a), calcined at 473 K (b), 723 K (c), 773 K (d), 823 K (e), 873 K (f), 923 K (g), 973 K (h), 1023 K (i), 1173 K (j), and 1373 K (k).

stretching of PO_3 terminal groups from pyrophosphate. The 925 cm^{-1} band could be assigned to symmetric stretching vibrations of PO_3 groups, while two bands at 622 and 522 cm^{-1} were regarded as deformation modes of PO_2 and PO_3 groups [6]. As the calcination temperature increased from 723 to 773 K, the band observed at 925 cm^{-1} shifted to 950 cm^{-1}, and a new small band appeared at 993 cm^{-1}. The above shift corresponded to the crystallization of pyrophosphate and the additional peak was attributed to the formation of orthophosphate. In the range of the calcination temperatures between 823 and 1023 K, the patterns both of metaphosphate and orthophosphate were recognized in the FT-IR spectra. The bands from metaphosphate were observed at 1270, 1158, 954, 774, and 470 cm^{-1} [6,7] and those from orthophosphate were assigned at 1093, 1058, 993, 622, 570, and 532 cm^{-1} [8,9], respectively. The sample calcined at 1173 K almost indicated the only pattern of orthophosphate.

Fig. 4 shows Raman spectra of the as-prepared and the calcined cerium phosphate samples. In the Raman spectra of the amorphous materials, four bands were observed at 1007, 627, 578, and 498 cm^{-1}. The principal broad band at 1007 cm^{-1} was assigned to the symmetric stretching of PO_3 terminal groups from pyrophosphate [10]. The bands at 627 and 498 cm^{-1} corresponded to the asymmetric and symmetric deformation modes of PO_4, and the one at 578 cm^{-1} was attributed to the deformation mode of PO_3 group. Calcinations at higher temperatures above 773 K promoted the main peak shift from 1007 to 1037 cm^{-1}, and at 823 K, several new peaks appeared. The 940 and 780 cm^{-1} peaks were due to the asymmetric and symmetric motions of the bridging oxygen in P–O–P unit of pyrophosphate [11]. The 971 cm^{-1} band was attributed to symmetric stretching of PO_4, and the bands between 300 and 500 cm^{-1} were due to the deformation of PO_3 group of orthophosphate. After the calcinations above 823 K, the peaks of pyrophosphate gradually disappeared and new bands attributed to metaphosphate and orthophosphate were produced. The peaks of former were observed at 1265, 1178, and 694 cm^{-1} and those of the latter were at 1074, 1056, 1028, 995, and 971 cm^{-1}, respectively [12,13]. The bands at 1265 and 1178 cm^{-1} were assigned to symmetric and asymmetric stretching of PO_2 group, and the 694 cm^{-1} peak was corresponded to symmetric motion of the bridging oxygen in P–O–P unit of metaphosphate. After calcination at 1373 K, the only peaks corresponding to orthophosphate were observed. The band at 971 cm^{-1} was due to the symmetric stretching of the PO_4 unit and those at 995 and 1028 cm^{-1} were attributed to the asymmetric stretching of the PO_4 group. The bands at 1056 and 1074 cm^{-1} were from the splitting of the asymmetric stretching mode of the PO_4 group [13].

3.2. Thermal behavior of the amorphous terbium phosphate

Fig. 5 shows the XRD patterns of the as-prepared and the calcined terbium phosphate samples. In contrast to the results of cerium phosphate, crystallization of amorphous terbium phosphate occurred at higher 973 K to produce a mixture of crystalline terbium orthophosphate ($TbPO_4$) and tetraphosphate ($Tb_2P_4O_{13}$). The tetraphosphate phase decomposed at 1673 K into a mixture of TbP_3O_9 and $TbPO_4$.

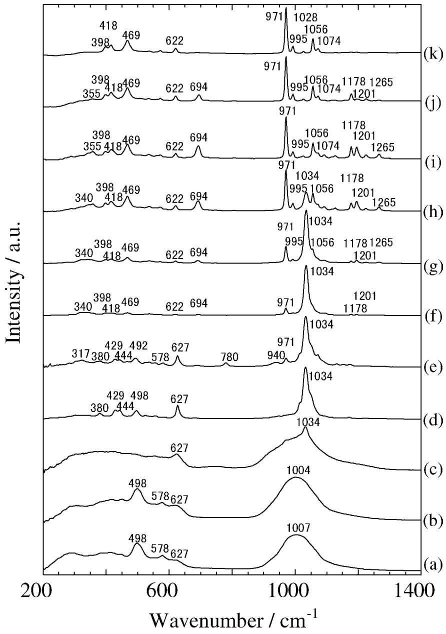

Fig. 4. Raman spectra of cerium phosphate calcined at various temperatures: as-prepared (a), calcined at 473 K (b), 723 K (c), 773 K (d), 823 K (e), 873 K (f), 923 K (g), 973 K (h), 1023 K (i), 1173 K (j), and 1373 K (k).

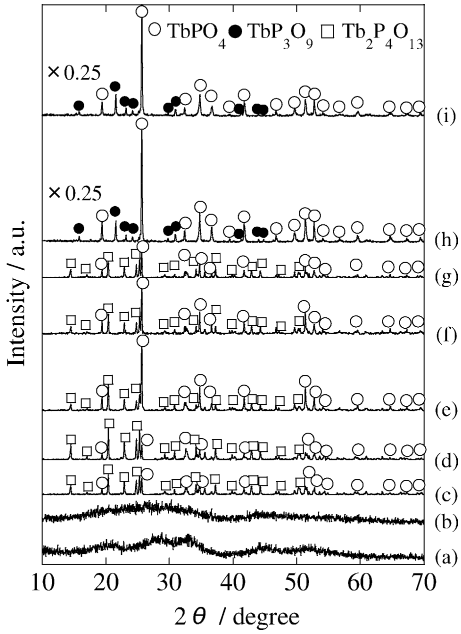

Fig. 5. XRD patterns of terbium phosphate calcined at various temperatures: as-prepared (a), calcined at 873 K (b), 973 K (c), 1073 K (d), 1373 K (e), 1423 K (f), 1473 K (g), 1673 K (h), and 1873 K (i).

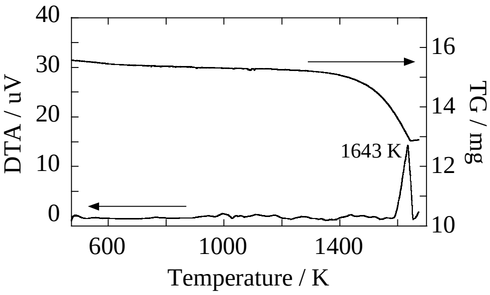

Fig. 6. TG–DTA spectra of terbium phosphate dried at 573 K.

Even after the calcination at 1873 K, the two-phase mixture remained and no single phase was obtained.

TG–DTA spectra of the amorphous terbium phosphate dried at 573 K are presented in Fig. 6. In the DTA curve, an exothermic peak was observed at 1643 K, which was corresponding to the decomposition of the tetraphosphate described above. The accompanying weight loss observed around 1600 K came from the volatilization of phosphorus oxide produced by the decomposition of the tetraphosphate.

Fig. 7 depicts the FT-IR spectra of the as-prepared and the calcined terbium phosphate samples. In the amorphous terbium phosphate, several broad bands were observed. As the calcination temperature increased, these broad bands sharpened accompanying the shift to higher wave numbers. The bands observed at 748 and 923 cm^{-1} in the amorphous sample were assigned to symmetric and asymmetric stretching of P–O–P group, which shifted to 760 and 957 cm^{-1} after the heating at 973 K. The band at 557 cm^{-1} was the deformation mode of PO_3 in pyrophosphate group. The increase in the calcination temperature induced the splitting of this band into several ones because of the deformation of the PO_2 and PO_4 groups in tetra and orthophosphate, respectively. Consequently, the peaks based on tetraphosphate were observed at 1313, 1258, 1182, 1102, 1034, 958, 795, 757, 684, 636, 560, 502, and 461 cm^{-1} [14], and those from orthophosphate were assigned at 957, 634, and 524 cm^{-1} [9]. Above 1673 K, the tetraphosphate was disappeared and the new bands from trimetaphosphate appeared at 1249, 1058, and 1019 cm^{-1}. These peaks corresponded to asymmetric stretching of PO_2, symmetric stretching of PO_2, and asymmetric stretching of P–O–P group, respectively [6,7].

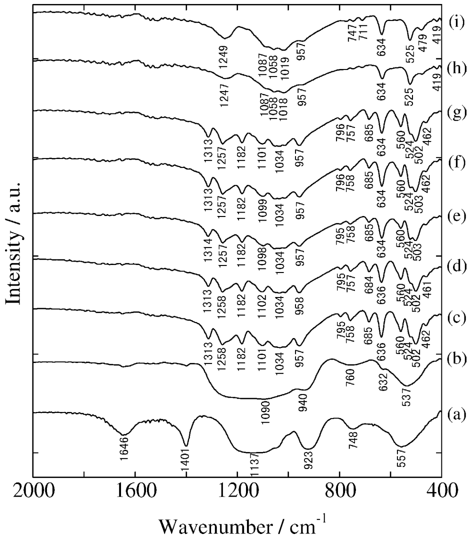

Fig. 7. FT-IR spectra of terbium phosphate calcined at various temperatures: as-prepared (a), calcined at 873 K (b), 973 K (c), 1073 K (d), 1373 K (e), 1423 K (f), 1473 K (g), 1673 K (h), and 1873 K (i).

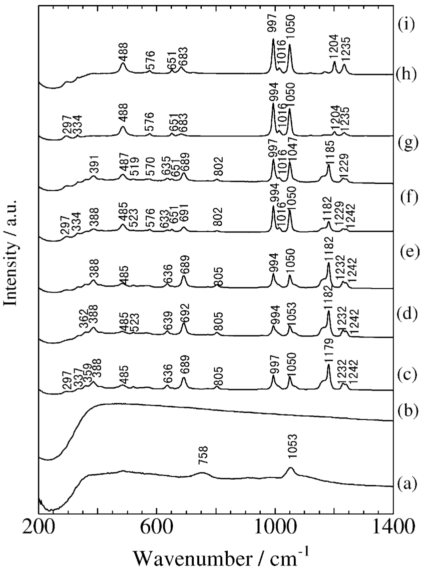

Fig. 8. Raman spectra of terbium phosphate calcined at various temperatures: as-prepared (a), calcined at 873 K (b), 973 K (c), 1073 K (d), 1373 K (e), 1423 K (f), 1473 K (g), 1673 K (h), and 1873 K (i).

The Raman spectra of terbium phosphate calcined at various temperatures are illustrated in Fig. 8. In amorphous state, a considerable broad band was observed. In the samples calcined between 973 and 1473 K, the bands of $TbPO_4$ were observed at 1050, 1016, 997, 636, 576, and 485 cm^{-1} [13], as well as those of $Tb_2P_4O_{13}$ at 1232, 1182, 804, and 689 cm^{-1} [15]. The band at 997 cm^{-1} corresponded to the symmetric stretching and those observed at 1016 and 1050 cm^{-1} were associated with the asymmetric stretching of the PO_4 group. The peaks at 1182 and 1232 cm^{-1} were assimilated to the symmetric and asymmetric of PO_2 and those at 689 and 804 cm^{-1} came from the symmetric and asymmetric of P–O–P bridges. After the calcination above 1673 K, the bands for stretching of P–O–P bridges and PO_2 group in trimetaphosphate were observed at 683, 1204 and 1235 cm^{-1}, which means the structural change from tetraphosphate to trimetaphosphate. The bands at 1235 and 1204 cm^{-1} were corresponding to the symmetric and asymmetric stretching of PO_2 group [7,13] and the 694 cm^{-1} band was due to the symmetric stretching of P–O–P group in trimetaphosphate.

3.3. Comparison of cerium and terbium phosphate

In comparison with the thermal behavior between cerium and terbium phosphate, two clear differences were recognized. First, the crystallization temperature of amorphous terbium phosphate was higher than that of cerium phosphate. According to the results of Raman spectra of these amorphous phosphates, larger value of the P–O stretching wave number was observed in terbium phosphate ($1053\,\mathrm{cm}^{-1}$) than in cerium phosphate ($1007\,\mathrm{cm}^{-1}$). This indicates that stronger P–O bond is formed in the amorphous terbium phosphate, and therefore higher temperature was required to rearrange atoms for crystallization.

The second difference is that orthophosphate single phase was obtained only in cerium phosphate, while in the case of terbium phosphate, a mixture of orthophosphate and trimetaphosphate was obtained after the high temperature calcinations. Since the standard formation enthalpy of cerium orthophosphate ($-1954\,\mathrm{kJ\,mol}^{-1}$) is lower than that of terbium ($-1925\,\mathrm{kJ\,mol}^{-1}$), it is considered that the production of orthophosphate single phase is easier in the case of cerium than terbium [16].

4. Conclusions

Amorphous cerium phosphate maintained its structure up to 723 K and it crystallized at 773 K to form a mixture of cerium pyrophosphate and orthophosphate, which means that these phases are the most stable crystalline phases at low temperatures. Heating at higher temperatures promoted the phase change from pyrophosphate to orthophosphate with the formation of metaphosphate, and only a single phase of $CePO_4$ was obtained at above 1173 K.

Crystallization of amorphous terbium phosphate occurred at 973 K to form a mixture of terbium orthophosphate and tetraphosphate. The tetraphosphate phase decomposed at 1673 K to produce a mixture of TbP_3O_9 and $TbPO_4$. The mixture of these compounds was stable even after the calcination at 1873 K, and therefore no single phase was obtained.

It has been recognized that amorphous cerium phosphate is easier to crystallize than terbium phosphate due to the difference of P–O bond strength in these phosphates. In addition, cerium phosphate tends to form a single phase of orthophosphate at high temperatures because of the more negative standard formation enthalpy than that of terbium phosphate.

Acknowledgements

The present work was partially supported by a Grant-in-Aid for Scientific Research Nos. 13555241 and 15550172 from The Ministry of Education, Science, Sports, and Culture, Japan. The authors sincerely thank Dr. Kuniaki Murase and Prof. Dr. Yasuhiro Awakura (Kyoto University) for their assistance with the Raman spectra measurements. This work was supported by the Industrial Technology Research Grant Program in 02 (Project No. 02A27004c) from the New Energy and Industrial Technology Development Organization (NEDO) based on funds provided by the Ministry of Economy, Trade and Industry, (METI) Japan.

References

[1] V. Mehta, G. Aka, A.L. Dawar, A. Mansingh, Opt. Mater. 12 (1999) 53.
[2] K. Riwotzki, H. Meyssamy, A. Kornowski, M. Haase, J. Phys. Chem. B 104 (2000) 2824.
[3] N. Imanaka, T. Masui, H. Hirai, G. Adachi, Chem. Mater. 15 (2003) 2289.
[4] I.L. Von, E.J. Botto, Z. Baran, Anorg. Allg. Chem. 430 (1977) 283.
[5] T. Masui, H. Hirai, N. Imanaka, G. Adachi, Phys. Status Solidi (a) 198 (2003) 364.
[6] D. Ilieva, B. Jivov, G. Bogachev, C. Petkov, I. Penkov, Y. Dimitriev, J. Non-Cryst. Solids 283 (2001) 195.
[7] D. Ilieva, B. Jivov, D. Kovacheva, T. Tsacheva, Y. Dimitriev, G. Bogachev, C. Petkov, J. Non-Cryst. Solids 293–295 (2001) 562.
[8] S. Lucas, E. Champion, C. Penot, G. Leroy, D. Vernache-Assollant, Key Eng. Mater. 206–213 (2002) 47.
[9] A. Hezel, S.D. Ross, Spectochim. Acta 22 (1966) 1949.
[10] R.K. Brow, D.R. Tallant, W.L. Warren, A. McIntyre, D.E. Day, Phys. Chem. Glass 38 (1997) 300.
[11] N. Khay, A. Ennaciri, J. Alloys Comp. 323 (2001) 800.
[12] G.M. Begun, C.E. Bamberger, J. Raman Spectrosc. 13 (1982) 284.
[13] G.M. Begun, G.W. Beall, L.A. Boatner, W.J. Gregor, J. Raman Spectrosc. 11 (1981) 273.
[14] A.U. Amour, M. Kizilyalli, High Temp. Mater. Sci. 36 (1996) 77.
[15] C.T. Dinh, P.V. Huong, R. Olazcuaga, C. Fouassier, J. Opt. Adv. Mater. 2 (2000) 159.
[16] L.A. Marinova, V.N. Yaglov, Zhur. Fizich. Khim. 50 (1976) 802.